

# The boson-fermion model: An exact diagonalization study

M. Cuoco,<sup>1,2</sup> C. Noce,<sup>1,3</sup> J. Ranninger,<sup>2</sup> and A. Romano<sup>1</sup>

<sup>1</sup>Unità I.N.F.M. di Salerno, Dipartimento di Fisica "E. R. Caianiello",  
Università di Salerno, I-84081 Baronissi (Salerno), Italy

<sup>2</sup>Centre de Recherches sur les Très Basses Températures associé à l'Université Joseph Fourier,  
C.N.R.S., BP 166, 38042 Grenoble-Cédex 9, France

<sup>3</sup>Unità I.N.F.M. di Salerno - Coherentia

The main features of a generic boson-fermion scenario for electron pairing in a many-body correlated fermionic system are: i) a cross-over from a poor metal to an insulator and finally a superconductor as the temperature decreases, ii) the build-up of a finite amplitude of local electron pairing below a certain temperature  $T^*$ , followed by the onset of long-range phase correlations among electron pairs below a second characteristic temperature  $T_\phi$ , iii) the opening of a pseudogap in the DOS of the electrons below  $T^*$ , rendering these electrons poorer and poorer quasi-particles as the temperature decreases, with the electron transport becoming ensured by electron pairs rather than by individual electrons. A number of these features have been so far obtained on the basis of different many-body techniques, all of which have their built-in shortcomings in the intermediate coupling regime, which is of interest here. In order to substantiate these features, we investigate them on the basis of an exact diagonalization study on rings up to eight sites. Particular emphasis has been put on the possibility of having persistent currents in mesoscopic rings tracking the change-over from single- to two-particle transport as the temperature decreases and the superconducting state is approached.

PACS numbers: 74.20.-z, 74.78.Na, 74.20.Mn

## I. INTRODUCTION

A great interest has recently been devoted in condensed matter theory to models for interacting boson-fermion systems. Among the topics to which these models apply, we recall the hole pairing in semiconductors<sup>1</sup>, the isospin singlet pairing in nuclear matter<sup>2</sup>,  $d$ -wave hole and antiferromagnetic triplet pairing in the positive- $U$  Hubbard system<sup>3</sup> (and possibly also in the t-J model), and entangled atoms in squeezed states in molecular Bose-Einstein condensation in traps<sup>4</sup>.

In the present paper we consider a boson-fermion model (BFM) which captures a number of basic physical properties of strongly interacting many-body systems where resonant pair states of bosonic nature form inside a reservoir of fermions. This BFM was originally conceived as a possible alternative and extension to the idea of bipolaronic superconductivity<sup>5</sup> - a scenario for systems with extremely strong electron-phonon coupling where all the electrons exist in form of locally bound pairs of small polarons. Since in such a case of extreme antiadiabaticity the mobility of bipolarons is expected to be vanishingly small, they have to be considered, for all intents and purposes, as remaining localized rather than condensing into a superfluid phase. An alternative to this situation was to consider a case where the electron-phonon coupling is of intermediate strength, such that the energy of locally bound *isolated* bipolarons is comparable with the gain in energy of itinerant electrons. This leads to a scenario where two-electron states fluctuate between pairs of itinerant single-electron states close to the Fermi level and localized bipolaron states which pin this Fermi level. A detailed discussion on such a polaron-induced scenario

for this BFM has been given recently<sup>6</sup>. Treating the bipolarons as bosonic entities which commute with the fermionic electrons, the Hamiltonian for such a system is given by

$$H = (D - \mu) \sum_{i\sigma} c_{i\sigma}^{\dagger} c_{i\sigma} + (\Delta_B - 2\mu) \sum_i \left( \rho_i^z + \frac{1}{2} \right) + t \sum_{i \neq j, \sigma} c_{i\sigma}^{\dagger} c_{j\sigma} + g \sum_i \left( \rho_i^{\dagger} c_{i\downarrow} c_{i\uparrow} + \rho_i^{-} c_{i\uparrow}^{\dagger} c_{i\downarrow}^{\dagger} \right). \quad (1)$$

The bipolarons are treated here as on-site entities having hard-core boson features and thus are represented by pseudo-spin operators  $\{\rho_i^{\dagger}, \rho_i^{-}, \rho_i^z\}$ .  $c_{i\sigma}^{\dagger}$  and  $c_{i\sigma}$  denote the creation and annihilation operators of the itinerant electrons and  $g$  is the strength of the boson-fermion charge exchange interaction. The hopping integral for the itinerant electrons is given by  $t$  with a half bandwidth equal to  $D = zt$ ,  $z$  denoting the coordination number of the underlying lattice. The energy level of the hard-core bosons is denoted by  $\Delta_B$ . A common chemical potential  $\mu$  ensures the conservation of the total charge  $n_{tot} = n_{F\uparrow} + n_{F\downarrow} + 2n_B$  ( $n_B$  and  $n_{F\uparrow, \downarrow}$  denote the total number of the hard core-bosons and of the electrons with up and down spin states). This model has been studied by a number of different many-body techniques, such as self-consistent diagrammatic studies<sup>7</sup>, dynamical mean-field theory<sup>8</sup> and renormalization group techniques<sup>9</sup>. The main message of all these studies was that this model contained the following basic physical properties:

*Upon decreasing the temperature below a certain characteristic  $T^*$ , local electron pairing (not electron pair states!) begin to form and exist over a finite time as well as space interval. As a consequence of that, a pseu-*

dogap centered around the Fermi level opens up in the density of states (DOS) of the itinerant electrons. Electrical transport is being controlled by relatively well defined single-electron states above  $T^*$ , while below  $T^*$  the electrons get heavily damped. Upon further decreasing the temperature, the electron pairs become better and better defined quasi-particles and ensure the transport, eventually leading to a superconducting state controlled by phase fluctuations of the electron pairs. The resistivity, just before entering this superconducting state, resembles that of an insulator, since it is determined by the electrons with their pseudogap features.

In the present paper, we examine all these features within an exact diagonalization scheme, evaluating the static and dynamical properties of the BFM, by means of the Lanczos procedure extended to finite temperature<sup>10</sup>. This technique has been tested and successfully applied on different many-body systems of strongly correlated electrons<sup>11</sup>, and allows to determine the temperature dependence of various physical quantities, which, combined with dynamical properties, gives a complete information about the energy spectrum and excitations of the model under examination. In particular, within this scheme of computation the trace of thermodynamic expectation values is obtained by means of Monte Carlo sampling, while for the determination of the relevant matrix elements the Lanczos method is used.

We restrict ourselves to the symmetric case, where the bosonic level lies in the middle of the electronic band, i.e.,  $\Delta_B = 0$ . For a different position of the bosonic level the physics is qualitatively the same, the relevant parameter in this scenario being the concentration of the bosons. Due to their hard-core nature, they induce correlation effects which lead to qualitative changes in the physical properties as we go from low ( $\bar{n}_B \geq 0$ ) to high ( $\bar{n}_B \simeq 0.5$ ) boson concentrations.

Our local phase space being made up of eight states, a large computational memory is required. This limits the present study to maximally eight sites systems if the evaluation of the static and dynamical quantities does not involve transitions between subspaces with a different number of fermions and bosons. Moreover, for the study of the spectral functions for the fermions, together with the previous constraint we have to consider a situation such that the discrete energy spectrum of our finite size system has contributions as close as possible to the Fermi level, in order to track the low energy features of interest here. Having the Fermi level lie in the center of the fermionic band (in order to avoid effects coming from any particular band structure), the maximal size of the system which we could consider is restricted to four sites rings allowing any concentration of fermions and bosons. As far as concerns the boson spectral function, we can investigate up to six sites rings since the constraint on the physical description of the fermionic properties does not apply.

The relevant correlation functions determining the onset of local electron pairing and spatial phase correla-

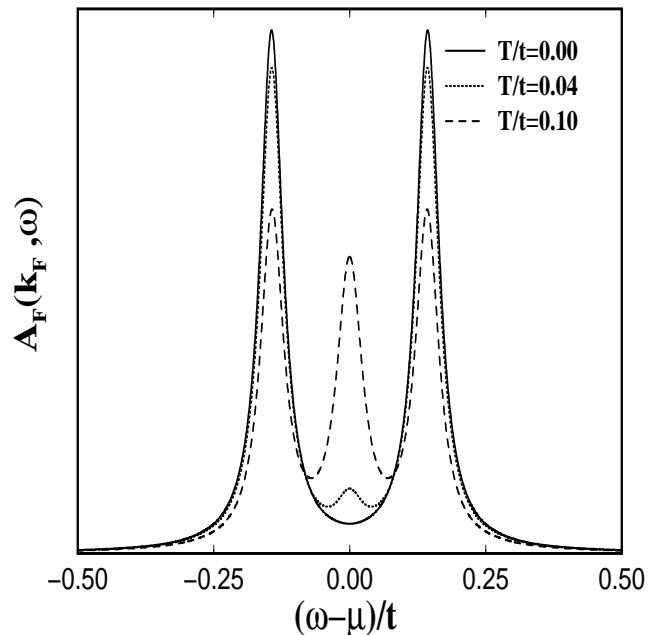


FIG. 1: Variation with temperature of the fermionic spectral function at the Fermi vector, evaluated for a 4-site ring with  $\Delta_B = 0$ ,  $g/t = 0.2$  and  $n_{tot} = 8$  ( $n_B = 2$ ).

tions are given by  $\langle \rho_i^+ c_{i\downarrow} c_{i\uparrow} + h.c. \rangle$  and  $\langle \rho_i^+ \rho_j^- \rangle$  and will be discussed in Section II. In Section III we examine the spectral properties of the hard-core bosons and compare them with the excitations of an equivalent XY model in the presence of a transverse field. The change-over from single-electron to electron pair transport will be discussed in Section IV on the basis of the temperature dependence of the optical conductivity and in section V in terms of persistent currents in mesoscopic rings.

## II. FROM LOCAL TO LONG-RANGE PHASE CORRELATIONS

The spectral features of the fermions are determined by

$$\begin{aligned}
 A_F(k, \omega) &= A_F^+(k, \omega) + A_F^-(k, -\omega) \\
 A_F^\pm(k, \omega) &= \Omega^{-1} \sum_{m,n} |\langle m | \begin{pmatrix} c_k^+ \\ c_k \end{pmatrix} | n \rangle|^2 e^{-\beta(E_n - \mu n_{tot})} \\
 &\quad \times \delta(\hbar\omega + 2\mu - E_m + E_n) \\
 \Omega^{-1} &= \sum_n e^{-\beta(E_n - \mu n_{tot})}, \quad (2)
 \end{aligned}$$

where  $A_F^\pm(k, \omega)$  represent the electron and hole spectral functions, respectively,  $\Omega$  denotes the partition function and  $E_m$  are the eigenvalues of the total Hamiltonian. In Fig. 1 we plot the evolution of the fermionic spectral function for electrons at the Fermi surface, i.e.,  $k = k_F$ .

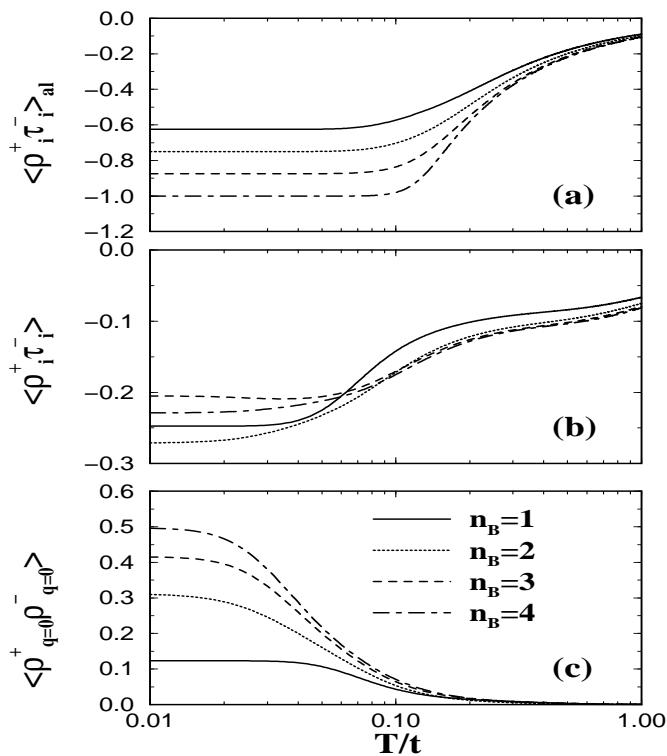


FIG. 2: Temperature dependence of the on-site correlation function  $\langle \rho_i^+ \tau_i^- \rangle$ , with  $\tau_i^- = c_{i\downarrow} c_{i\uparrow}$ , evaluated for a single site in the atomic limit (Fig. 1a). Comparison of this local correlation function (Fig. 1b) and  $\langle \rho_{q=0}^+ \rho_{q=0}^- \rangle$  (Fig. 1c), measuring the long-range phase coherence of the hard-core bosons, evaluated for an 8-site system for different boson concentrations  $n_B$ . The value of the boson-fermion coupling is  $g/t = 0.4$ .

We notice that with decreasing temperatures spectral weight is transferred from the Fermi energy to side bands which characterize the contributions from bonding and antibonding two-electron states. This emptying out of the spectral density near the Fermi energy is responsible for the opening of a pseudogap in the DOS of the fermions below a certain characteristic temperature  $T^*$ , which can be determined from the drop in spectral weight of  $A_F(k_F, \mu)$ .

The onset of local electron pairing, seen in the opening of a pseudogap in the electronic DOS, is manifest moreover in a strong increase of the local correlation function between the hard-core bosons and the electron pairs  $\langle \rho_i^+ c_{i\downarrow} c_{i\uparrow} \rangle$ . This effect is already inherent in a single-site system and is illustrated in Fig. 2a, showing a characteristic increase of this correlation function for temperatures of the order of  $g$ , which is the energy gain when they engage in a bonding state  $(1/\sqrt{2})[\rho_i^+ + c_{i\uparrow}^+ c_{i\downarrow}^+]|0\rangle$ . Going beyond the single-site case, this energy gain is reduced to  $g^2/t$  as a consequence of the electron itinerancy entering into competition with the charge exchange mechanism. The intensity of the on-site correlation between bosons and electron pairs then

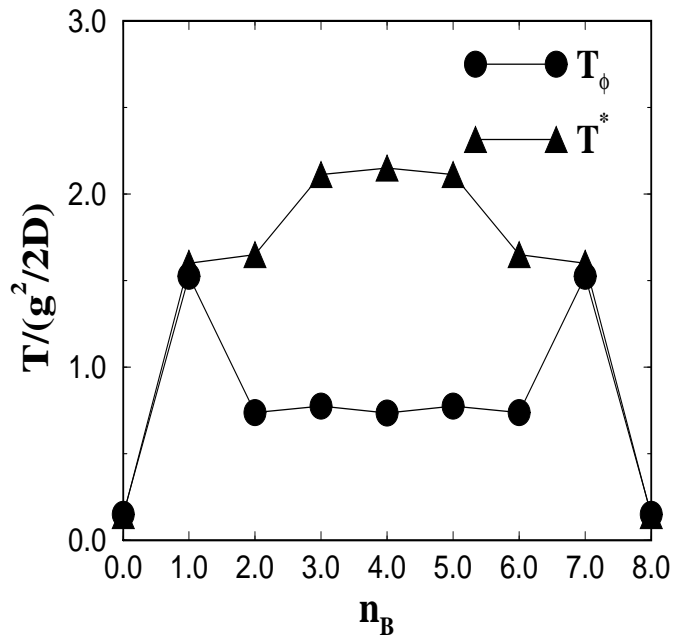


FIG. 3: Variation of  $T^*$  and  $T_\phi$  as a function of  $n_B$  for an 8-site ring with  $g/t = 0.4$  and  $n_{\text{tot}} = n_B + 8$ .

correspondingly decreases, as illustrated in Fig. 2b for different total numbers of charge carriers, corresponding to  $n_B = 1, 2, 3, 4$ . Finally, in Fig. 2c we examine the long-range phase coherence for the hard-core bosons, described by  $\langle \rho_{q=0}^+ \rho_{q=0}^- \rangle = (1/N) \sum_{\delta=1}^8 \langle \rho_i^+ \rho_{i+\delta}^- \rangle$ . We notice that this correlation function strengthens as  $T$  drops below a certain characteristic temperature  $T_\phi$  ( $< T^*$ ).

The evolution of  $T^*$  and  $T_\phi$  noticeably changes with the concentration of bosons. We derive these temperatures from the inflexion point of these two correlation functions and present them as a function of  $n_B$  in Fig. 3. While for small boson concentration  $T_\phi$  follows the same behavior as  $T^*$ , it begins to show a downwards trend upon further increasing the boson concentration. This confirms a recent result for the phase diagram of the BFM obtained within a diagrammatic technique which explicitly takes into account the hard-core nature of the bosons<sup>12</sup>. In that study it was concluded that this non-monotonic behavior of  $T_\phi$  should be related to the correlation effects in the hard-core boson subsystem, leading to an increasingly heavy mass of the bosons as their concentration approaches the dense limit, i.e.,  $n_B = 0.5$ . This is to be expected for systems where the onset temperature of phase ordering is related to the phase stiffness  $D_\phi \simeq n_p/m_p$  of the electron pairs which is induced by the boson-fermion exchange coupling,  $n_p = \langle n_{F\uparrow} n_{F\downarrow} \rangle - \langle n_{F\uparrow} \rangle \langle n_{F\downarrow} \rangle$  denoting their density and  $m_p$  their mass.

### III. BOSON SPECTRAL PROPERTIES: A COMPARISON WITH XY PHASE FLUCTUATION SCENARIOS

After having considered the spectral properties of the fermions in the preceding section, let us now discuss the spectral properties of the hard-core bosons. The appropriate spectral function in this case is

$$\begin{aligned} A_B(q, \omega) &= A_B^+(q, \omega) - A_B^-(q, \omega) \\ A_B^\pm(q, \omega) &= \Omega^{-1} \sum_{m,n} |\langle m | \rho_q^\pm | n \rangle|^2 e^{-\beta(E_n - \mu n_{tot})} \\ &\quad \times \delta(\hbar\omega + 2\mu - E_m + E_n), \end{aligned} \quad (3)$$

with  $\rho_q^\pm = \frac{1}{\sqrt{N}} \sum_i e^{iqr_i} \rho_i^\pm$ . We ultimately want to compare this spectral function, evaluated within the BFM, with that of an effective XY model in a transverse field, described by

$$H_{XY} = -J \sum_{i,\delta} \rho_i^+ \rho_{i+\delta}^- + h \sum_i \left( \rho_i^z + \frac{1}{2} \right). \quad (4)$$

The corresponding results are presented in Fig. 4, showing the absolute values of these correlation functions (we recall that they are negative for negative frequencies  $\omega$ ). For the case considered here, a 6-site ring with 3 bosons and  $\Delta_B = 0$ , we have a chemical potential  $\mu = 0$  and thus we choose  $h = 0$  in order to describe an equivalent physical situation within a XY model. The typical energy scale of the bosonic excitations is of the order of  $g^2/2D$  which is the energy scale related to the exchange interaction allowing the transfer of a boson from a given site to an adjacent one. The strong similarity between these two spectral functions over the entire range of  $q$  vectors is a strong indication that for low temperatures ( $T = 0$  in the present case) the excitation spectrum of the BFM is determined by phase fluctuations of the bosonic charge carriers.

In Fig. 5 we illustrate for the fully symmetric case ( $\Delta_B = 0$  and  $n_{tot} = 12$  for a 6-site ring) how the spectral function of the hard-core bosons evolves as a function of temperature. We notice that upon increasing the temperature above  $T_\phi$ , this spectral function becomes more and more incoherent. The quasi-particle features of the fermions and of the hard-core bosons develop in opposite directions as the temperature is lowered. Above  $T^*$  the fermions are still rather well defined quasi-particles, while the hard-core bosons are completely incoherent. Between  $T^*$  and  $T_\phi$  the fermions lose their quasi-particle features, while those of the bosons are getting better and better defined. Finally, below  $T_\phi$  the only good quasi-particles are the hard-core bosons and consequently also the local electron-pairs. This change in the quasi-particle features from single to two-particle states will become more apparent in the transport properties, discussed in the following Section.

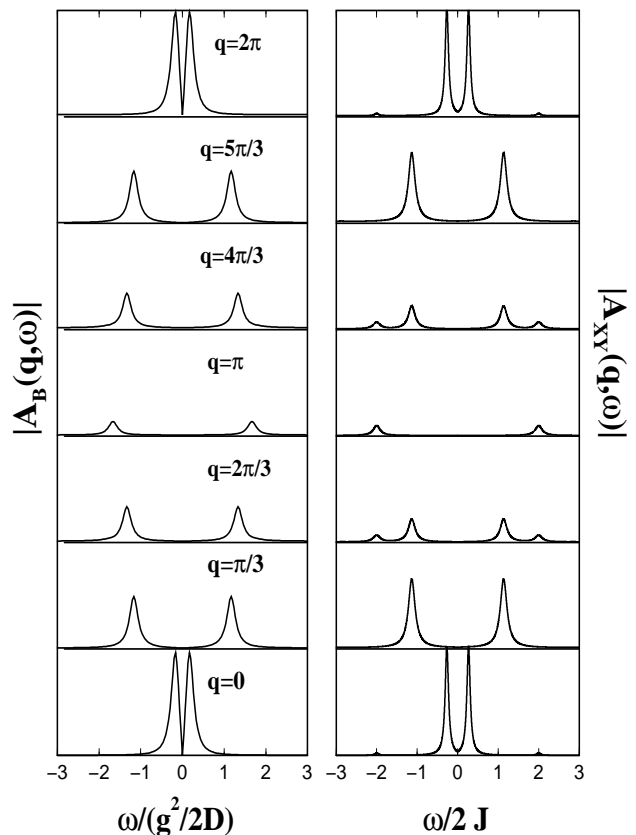


FIG. 4: Comparison at  $T = 0$  of the boson spectral function  $A_B(q, \omega)$  for  $n_{tot} = 12$  ( $n_B = 3$ ) on a 6-site ring with the spectral function of an equivalent XY model (denoted by  $A_{XY}(q, \omega)$ ).

### IV. FERMION VERSUS BOSON TRANSPORT

The spectral properties of the fermionic single-particle excitations, examined in Section II, indicate a loss of spectral weight for wave vectors centered around  $k_F$ , which is responsible for the opening of the pseudogap in the DOS. Full many-body calculations, involving self-energy corrections<sup>7,8</sup>, have shown that besides this loss of spectral weight, fermions also lose their quasi-particle features below  $T^*$ . They become purely diffusive and show up in a resistivity which monotonically increases as the temperature tends to zero. At the same time, the bosons and respectively the electron pairs, which are diffusive above  $T^*$ , become well defined quasi-particles upon approaching  $T_\phi$ , as discussed in section III. Thus, the bosonic charge carriers with charge  $2e$  are expected to ensure the transport upon approaching  $T_\phi$  and eventually lead to a drop in the resistance and ultimately to a superconducting state.

These features can be illustrated within the present exact diagonalization study in terms of the optical conductivity arising from the fermions and the bosons, respectively. The electric field in the present model

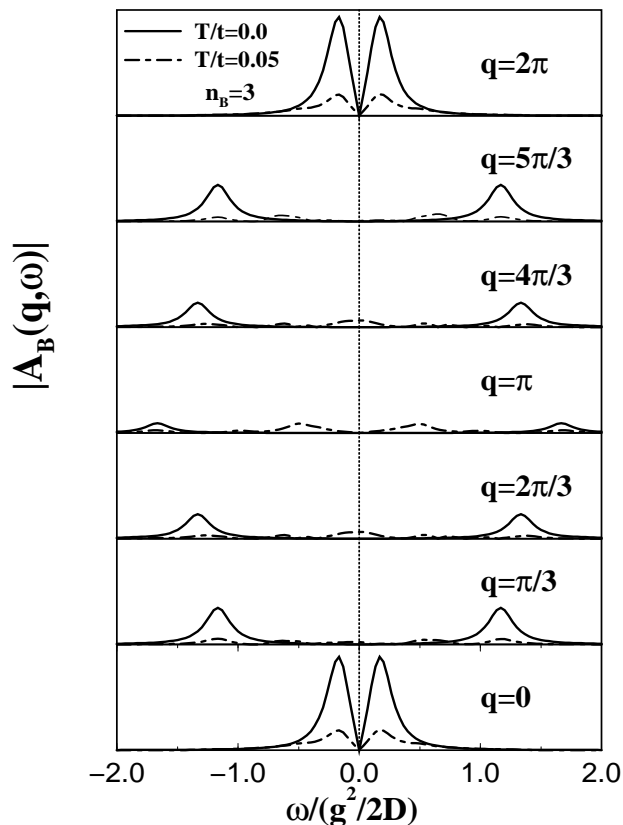


FIG. 5: Evolution with temperature of the spectral properties of the hard-core bosons for a 6 site ring with 3 bosons ( $n_{tot} = 12$ ) for two temperatures below and above  $T_\phi$ .

couples exclusively to the fermions, since the bosons are intrinsically localized. Nevertheless, because of the boson-fermion exchange coupling the bosons, and consequently also the fermion pairs, acquire itinerancy (as shown in Section III) and thus contribute to the transport via an Aslamazov-Larkin type contribution to the conductivity<sup>13</sup>. In order to capture this effect within the present exact diagonalization study, we decompose the current carried by the fermions  $j_F = t \sum_{i,\delta,\sigma} (c_{i,\sigma}^+ c_{i+\delta,\sigma} - h.c.)$  into a term associated with a current carried by the bosons  $j_B = t_B \sum_{i,\delta} (\rho_i^+ \rho_{i+\delta}^- - h.c.)$  plus a remainder  $\tilde{j}_F$  such that

$$j_F(t) = j_B(t) + \tilde{j}_F(t). \quad (5)$$

Separating optimally the contributions coming from the current-current correlation function for the bosons from the remainder of the fermions, we require  $\langle j_B(t) \tilde{j}_F(t) \rangle = 0$ , which defines an effective boson hopping integral as  $t_B = \langle j_F(t) j_B(t) \rangle / \langle j_B^2(t) \rangle$ . Such a decomposition is meaningful in a situation where the current transported by the fermions is rapidly dissipated as a function of time, described by  $\langle \tilde{j}_F(t) \tilde{j}_F(t') \rangle$ , and its long time behavior is getting controlled by the current transported by the bosons, described by  $\langle j_B(t) j_B(t') \rangle$ . Such a situation is

realized for low temperatures, around and below  $T_\phi$ . We can then safely neglect the contributions coming from the cross terms  $\langle j_F(t) j_B(t') \rangle$ .

We report in Fig. 6a the optical conductivity coming from exclusively the single-electron transport, given by  $\langle j_F(t) j_F(t') \rangle$ , and in Fig. 6b the contribution coming from bosonic charge carriers. We notice that for the fermionic contribution  $\sigma_F(\omega)$  to the optical conductivity we obtain a featureless metallic-type behavior for  $T > T^*$  ( $T/t = 0.3$  in our case), while upon going below  $T^*$ , a pseudogap structure materializes. Upon further decreasing the temperature below  $T_\phi$ ,  $\sigma_F(\omega)$  shows a well developed gap, reflecting the onset of an insulating behavior, as it can be inferred from the temperature behavior of the *dc* conductivity, illustrated in the inset of Fig. 6a.

At the same time, when sweeping through this same temperature interval, we notice the build-up of a structured contribution in the bosonic component of the optical conductivity  $\sigma_B(\omega)$ , which develops precisely in the frequency interval where the pseudogap appears in the fermionic contribution  $\sigma_F(\omega)$ . These features confirm the cross-over from fermionic to bosonic transport with decreasing temperature.

Of course, the spectral weight of the bosonic absorption is much smaller with respect to that of the fermionic sector. The effective boson hopping is  $t_B \sim g^2/2D$ , and hence the relative spectral weight of the bosonic absorption goes like  $\sim t_B^2$ . Nevertheless, it becomes clear from Fig. 6 that below  $T_\phi$  the transport at low frequency ( $\omega/t < g^2/2D$ ) is completely due to bosons and pairs of fermions.

## V. PERSISTENT CURRENTS IN MESOSCOPIC RINGS

The change-over between single-particle and two-particle transport is a salient feature of the BFM and its experimental verification would be vital in verifying such a scenario. As we have seen above, the onset of bosonic transport is not necessarily linked to a superconducting state. It is sufficient to have phase-coherent free particle-like bosonic excitations. In mesoscopic rings where persistent currents are a characteristic feature<sup>14</sup>, it should be possible to detect this change-over in transport when threading a magnetic flux through such a ring. This can give rise to persisting currents, periodically varying as a function of the flux  $\Phi$ . In units of the flux quantum  $\Phi_0 = \hbar c/e$  this periodicity should then be seen in multiples of  $\Phi/\Phi_0 = n$  if the transport is via single electrons, and of  $\Phi/\Phi_0 = n/2$  if it is due to two-particle bosonic transport,  $n$  denoting an integer number.

We investigate this problem in the standard way by evaluating the free energy  $F(\Phi)$  in the presence of a magnetic field and then determine the resulting current as  $J/N = \partial F(\Phi)/\partial \Phi$ . The behavior of  $F(\Phi)$  follows from the evaluation of the thermal average of the Hamiltonian (1), upon making the Peierls substitution

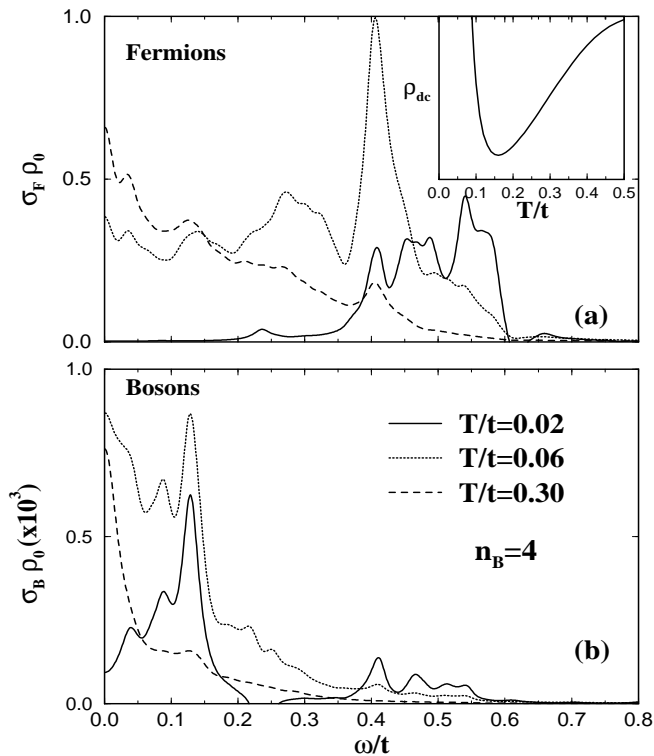


FIG. 6: Optical conductivity due to fermions (Fig. 4a) and due to bosons (Fig. 4b) for an 8-site ring with  $n_{tot} = 16$  ( $n_B = 4$ ) and three characteristic temperatures, corresponding to above  $T^*$ , between  $T^*$  and  $T_\phi$  and below  $T_\phi$ . The displayed difference in the amplitude of the fermionic and bosonic conductivity is set by the ratio between the effective boson and fermion hopping ( $\sim g^2/2D$ ). The scale is fixed by  $\rho_0 = \hbar a/e^2$  where  $a$  is the atomic distance.

$t \rightarrow t \exp\left(-i\frac{\Phi}{N\Phi_0}\right)$ . We illustrate in Fig. 7 the variation in the ground state of  $F(\Phi)$  as a function of  $\Phi/\Phi_0$  for the uncoupled system ( $g = 0$ ) and the fully interacting system ( $g \neq 0$ ). In the inset of the figure we also report the behavior of  $F(\Phi)$  for small positive values of  $\Phi$  at  $T = 0$  and at a finite temperature  $T > T_\phi$ , in the case  $g/t = 0.4$ . As to be expected, for the case  $g = 0$  we find a situation where the applied field lowers the energy of the system, arriving at minima at  $\Phi/\Phi_0 = n/2$  (see dotted line in Fig. 7). The periodicity of one flux quantum of  $F(\Phi)$  suggests that the effect of the flux is to introduce a paramagnetic current made out of single-electron states. Upon switching on the boson-fermion interaction,  $g \neq 0$ , one finds that around  $\Phi = 0$  the free energy below  $T_\phi$  increases with increasing  $\Phi$  before bending over and following essentially the same behavior as that obtained for  $g = 0$ . This suggests that if a small flux is applied to the system, a diamagnetic screening current is building up which, eventually, gives way to a paramagnetic current stabilizing the system when the flux is further increased. Hence, upon switching on the boson-fermion interaction,

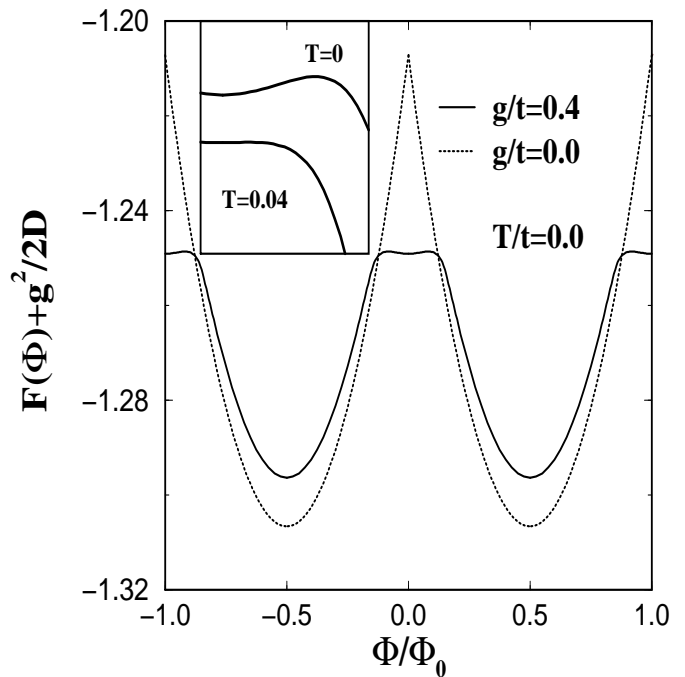


FIG. 7: Comparison of the free energy  $F(\Phi)$  as a function of the flux  $\Phi$  for the uncoupled ( $g = 0$ ) and the coupled ( $g \neq 0$ ) boson-fermion system. In the inset we present the evolution of  $F(\Phi)$  for small positive values of  $\Phi$  at  $T = 0$  and  $T = 0.04$  ( $> T_\phi$ )

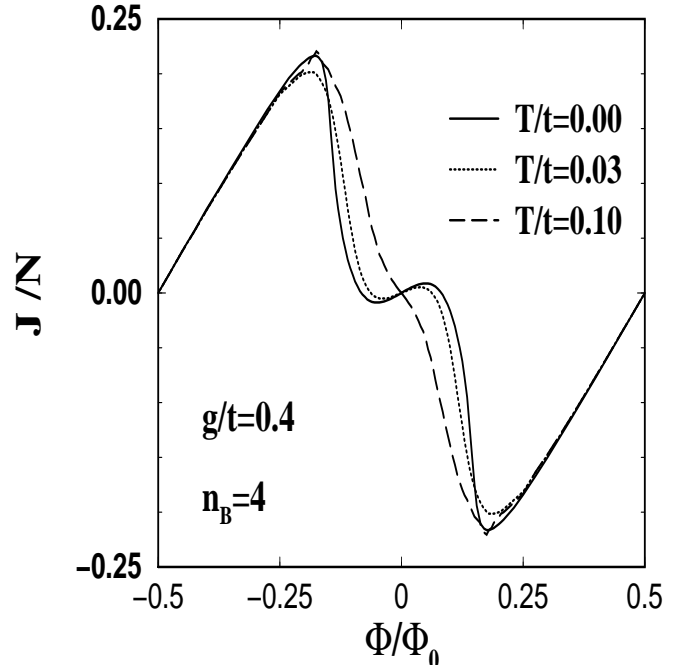


FIG. 8: Evolution with temperature of the current induced by a magnetic field threading a mesoscopic ring, illustrating the change in periodicity of the current as we pass from temperatures above  $T_\phi$  to below it.

the system evolves towards a state where the free energy exhibits minima at values of the flux with periodicity  $\Phi_0/2$ . This is indicative of an induced current made out of carriers having charge  $2e$ , and of an off-diagonal long-range order in the ground state. These conclusions are based on results derived a long time ago<sup>15,16</sup> in order to provide a criterion to distinguish between normal and superconducting ground states from the functional form of  $F(\Phi)$ , without any knowledge of the symmetry of pair-pair correlation functions. The fact that the minimum of the free energy at  $\Phi/\Phi_0 = 0$  is not the same as at  $\Phi/\Phi_0 = 1/2$  is due to the finite-size calculation presented here, analogous to the study of the anomalous flux quantization in the negative  $U$  Hubbard problem (see Fig. 1 in ref.<sup>17</sup>). As the temperature is increased above  $T_\phi$ , we notice that the minimum of  $F$  at  $\Phi = 0$  gradually disappears, thus stabilizing the paramagnetic single-electron current.

In Fig. 8 we present the current induced by the magnetic flux threading an 8-site mesoscopic ring as a function of  $\Phi/\Phi_0$ , for three characteristic temperatures, two below and one above  $T_\phi$ . We again can see the change-over from two-particle to single-particle transport. Experiments on mesoscopic ring made out of a high- $T_c$  compound might possibly have seen such two-particle transport at low temperatures<sup>18</sup>.

## VI. CONCLUSIONS

The present exact diagonalization study of the BFM confirms previous results obtained by various many-body techniques, all of which have their built-in shortcomings. The competitive effect of local and long-range correlations is a new element in the present approach, allowing

to extract some relevant physics underlying the BFM. They are characterized by the energy scales  $k_B T^*$  and  $k_B T_\phi$ , describing respectively the onset of local pairing and the establishment of a phase-correlated state on a long range, the latter being indicative of a superconducting phase in an infinite system. The change-over from single-particle to two-particle transport is most clearly seen and discussed in terms of the optical conductivity, showing below  $T^*$  a single-particle pseudogap feature together with a two-particle contribution developing in the frequency window opened up by the pseudogap. A clear-cut experiment for verifying the present scenario would be to study the change-over from single-electron to two-electron transport in mesoscopic rings, the theoretical expectations for which have been discussed.

In the present study, we limited the analysis to the case of optimal resonant scattering between the electrons and the local bound electron pairs, this being the physically most interesting case for the interplay between phase and amplitude fluctuations. Such a situation is realized when the bosonic level  $\Delta_B$  lies in the middle of the fermionic band (i.e.  $\Delta_B = 0$ ). By changing the position of the bosonic level, there are no qualitative changes as far as concerns the static and dynamical response and the appearance of two characteristic energy scales which control the short and long range phase coherence. In particular, the three-peak structure in the density of states (Fig. 1) remains the same, but the spectral weight is now asymmetric with respect to the chemical potential.

## ACKNOWLEDGMENTS

M.C. acknowledges support from Marie Curie Fellowship within the Program "Improving Human Potential".

- 
- <sup>1</sup> A. Mysyrowicz, E. Benson, and E. Fortin, Phys. Rev. Lett. **77**, 896 (1996).  
<sup>2</sup> A. Schnell, G. Roepke, and P. Schuck, Phys. Rev. Lett. **83**, 1929 (1999).  
<sup>3</sup> E. Altman and A. Auerbach, Phys. Rev. B **65**, 104508 (2002).  
<sup>4</sup> V. A. Yurovski and A. Ben-Reuven, cond-mat/0205267.  
<sup>5</sup> A. S. Alexandrov and J. Ranninger, Phys. Rev. B **23**, 1796 (1981).  
<sup>6</sup> J. Ranninger and A. Romano, Phys. Rev. B **66**, 094508 (2002).  
<sup>7</sup> J. Ranninger, J.-M. Robin, and M. Eschrig, Phys. Rev. Lett. **74**, 4027 (1995).  
<sup>8</sup> J.-M. Robin, A. Romano, and J. Ranninger, Phys. Rev. Lett. **81**, 2755 (1998).  
<sup>9</sup> T. Domanski and J. Ranninger, Phys. Rev. B **63**, 134505 (2001).  
<sup>10</sup> J. Jaklic and P. Prelovsek, Phys. Rev. B **49**, 5065 (1994).  
<sup>11</sup> J. Jaklic and P. Prelovsek, Adv. in Physics **49**, 1 (2000).  
<sup>12</sup> J. Ranninger and L. Tripodi, cond-mat/0212332.  
<sup>13</sup> P. Devillard and J. Ranninger, Phys. Rev. Lett. **84**, 5200 (2000).  
<sup>14</sup> M. Buttiker, Y. Imry, and R. Landauer, Phys. Lett. **96A**, 365 (1983).  
<sup>15</sup> N. Byers and C. N. Yang, Phys. Rev. Lett. **7**, 46 (1961).  
<sup>16</sup> C. N. Yang, Rev. Mod. Phys. **34**, 694 (1962).  
<sup>17</sup> C. A. Stafford and A. J. Millis, Phys. Rev. B **48**, 1409 (1993).  
<sup>18</sup> K. Kawabata, S. Tsukui, Y. Shono, O. Michikami, H. Sasakura, K. Yoshiara, Y. Kakehi, and T. Yotsuya, Phys. Rev. B **58**, 2458 (1998).